

Advanced Modeling of Distortion Effects in Bipolar Transistors Using the Mextram Model

Leo C. N. de Vreede, Henk C. de Graaff, Koen Mouthaan, *Student Member, IEEE*,
Marinus de Kok, Joseph L. Tauritz, *Member, IEEE*, and Roel G. F. Baets, *Member, IEEE*

Abstract—The modeling of distortion effects in bipolar transistors due to the onset of quasi-saturation is considered. Computational results obtained using the Mextram and Gummel-Poon models as implemented in a harmonic balance simulator are compared with measured results.

I. INTRODUCTION

IN MOBILE telecommunication receivers and transmitters there are several constraints on the power consumption and the supply voltage. These will, in general, lead to a limit on the collector emitter voltage. It is clear that at higher current levels or at a relatively low collector emitter voltage, the voltage drop over the epilayer of the collector can lead to forward biasing of the internal junction. This effect is called quasi-saturation (q.s.) and has been the subject of several publications: [1], [4]–[7], [9]–[11]. Quasi-saturation leads to current gain (β) and cut-off frequency (f_T) fall-off at higher current levels. Less well known to designers is the fact that the onset of q.s. also has a dominant influence on the distortion behavior of the bipolar transistor [9]. In conventional transistor models the modeling of q.s. is limited to the voltage drop over the fixed internal collector resistance (R_c), which can lead to “unexpected” results when realized circuits are measured. Quasi-saturation effects are of particular interest under high drive conditions, as in power stages or mixers.

When the internal base collector junction becomes forward biased, the injection of minority carriers in the epilayer leads to a strong reduction of the epilayer resistance and the build up of storage charge. This reduction of the epilayer resistance is described by Kull *et al.* [11] and more completely by de Graaff and Kloosterman [14], [18] who included a more precise description of the influence of space charge modulation due to hot carriers and current spreading. The latter leads to a more accurate description of the epilayer behavior in all operating modes [18]. We can model this reduction of the epilayer resistance by a current source which is controlled by two voltages, namely the internal junction voltage V_{b2c2} and the external voltage V_{b2c1} (see Fig. 1). The equations for I_{epi} depend on the chosen epilayer model: Kull or Mextram.

Fig. 2 shows the dc epilayer resistance ($R_{c1c2} = V_{c1c2}/I_{epi}$) behavior for the Kull Model (see Appendix). As can be noted from this figure the epilayer resistance is initially equal to RCV and increases due to the space charge modulation

Manuscript received February 24 1995; revised June 10, 1995.

The authors are with the Delft Institute for Microelectronics and Submicron Technology, Delft University of Technology, 2600 GA Delft, The Netherlands.
Publisher Item Identifier S 0018-9200(96)00102-3.

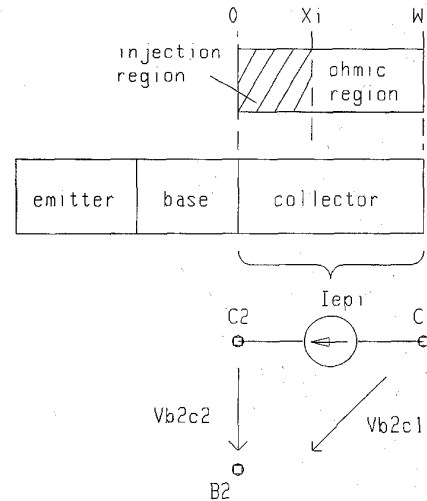


Fig. 1. Collector epilayer modeling with minority carrier injection.

(Kirk effect) until the internal junction voltage exceeds the built-in voltage VDC and q.s. sets in. It must be noted that the Kull model becomes inaccurate for a collector current $I_c \geq I_{HC} (= q \cdot A \cdot v_{lim} \cdot N_c)$.

The Mextram model release 503 [19] also includes hot carrier behavior and current spreading. The derivation of the epilayer current is given in [18]. The equations involved are given in the Appendix. Fig. 3 shows the epilayer resistance R_{c1c2} as function of the collector current for different external junction voltages V_{b2c1} . In this figure, the epilayer resistance once again is initially equal to the value of RCV; when the collector current reaches the hot carrier current the epilayer resistance will increase to a maximum value. This maximum is given by the Mextram parameter SCRCV which represents the space-charge limited epilayer resistance [18]. Note that the epilayer resistance decreases when the internal junction voltage exceeds the built-in voltage VDC. The parameters used in Figs. 2 and 3 are the same.

II. THE MODELING OF QUASI-SATURATION IN TRANSISTOR MODELS

In conventional transistor models such as the Spice implementation of the Gummel-Poon (GP) model [12] the voltage drop in the collector is modelled by a single ohmic resistor R_C (see Fig. 4). In the Mextram and Kull model the voltage drop

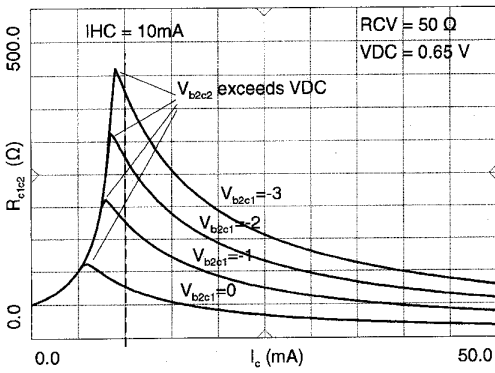


Fig. 2. Epilayer resistive behavior following Kull as function of the collector current for different external base collector voltages.

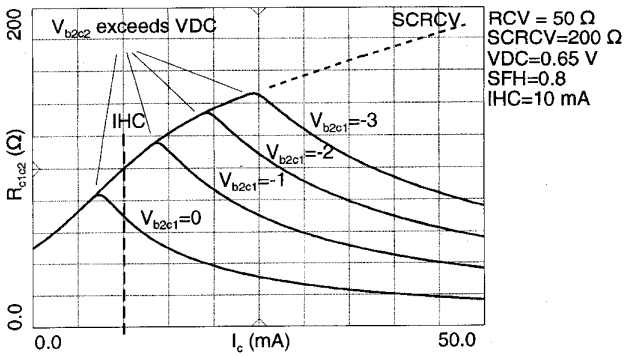


Fig. 3. Behavior of the epilayer resistance as function of the collector current for different external base collector voltages, based on the Mextram model.

in the collector region is modelled by the ohmic buried layer resistor RCC and a voltage-controlled current source I_{c1c2} (see Fig. 5). The controlled source is used to account for the voltage drop across the epilayer resistance, modulated by the injected storage charge in the collector region [14], [18]. The extra voltage drop in the Mextram model leads to earlier forward biasing of the internal base collector junction than in the Gummel-Poon model. This is best illustrated by considering the simulation results obtained using the Gummel-Poon and Mextram models for the same transistor. We have chosen the BFR520 transistor commonly employed in discrete RF circuits. Computed $I_c(V_{ce})$ characteristics are compared with measurement data in Fig. 6. The q.s. region ($V_{b2c2} \geq 0.7 \text{ V}$) is much larger for Mextram than for GP. Both models give a reasonable fit of the $I_c(V_{ce})$ characteristic, but GP does so by manipulating the Early voltages; GP however, fails to describe distortion behavior at higher current levels or at low collector emitter voltages, as will be explained in Section III.

III. HIGH CURRENT LOW FREQUENCY DISTORTION EFFECTS

Distortion effects at low current levels in bipolar transistors are well understood [2], [3], [8]. Conventional transistor models like Gummel-Poon [12] as well as the Mextram model can model most of the distortion effects for moderate drive conditions. At high current levels or at lower collector emitter

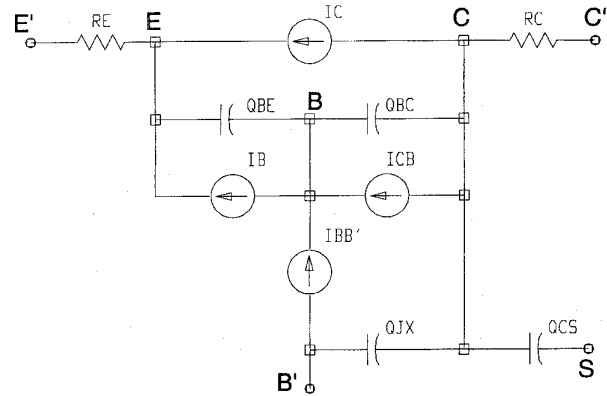


Fig. 4. The standard Gummel-Poon large signal model.

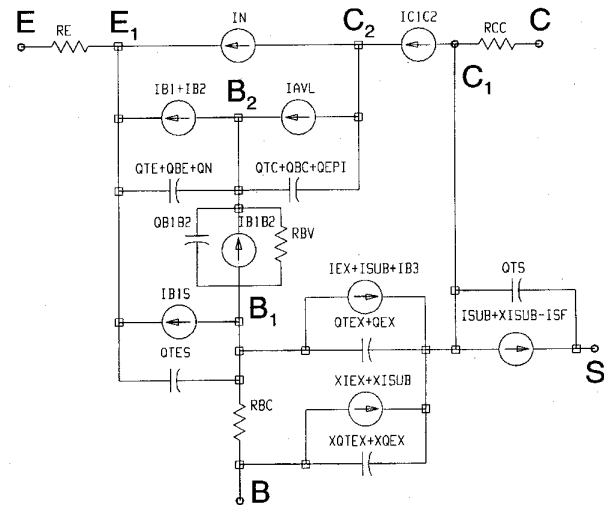


Fig. 5. The Mextram large signal model.

voltages q.s. will set in at a certain point for a given device. The onset of q.s. will lead to an increase in the third order distortion component [9].

Distortion Increase Due to q.s.

This increase in distortion is caused by the internal base collector junction becoming forward biased. When this happens the injection of minority carriers in the epilayer (related to the built-in base collector junction voltage) will lead to a substantial reduction of the epilayer resistance and the build up of storage charge. This, combined with the increase of the reverse component of the main current, will lead to a significant change in the small-signal transfer of the device under consideration. The distortion behavior can be understood by studying the small-signal transfer of the circuit in Fig. 7. At sufficiently low frequencies (ignoring reactive elements) the higher harmonics in the output of the transistor will be related to the input voltage by a Taylor series [12]. Consequently, the distortion behavior of a device at low frequencies can be studied for low driving conditions by investigating the

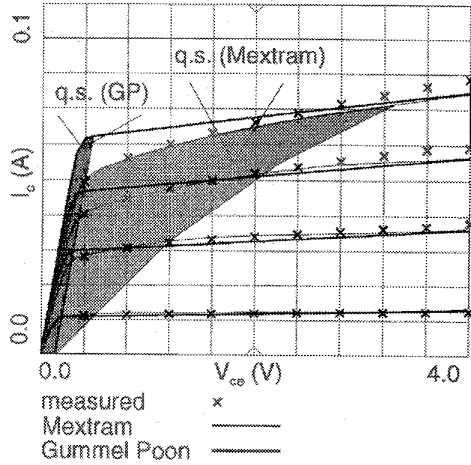


Fig. 6. $I_c(V_{ce})$ characteristics of the BFR520 transistor.

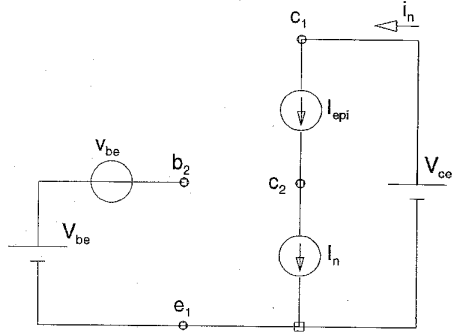


Fig. 7. Simplified circuit model of a bipolar transistor with a lightly doped epilayer.

derivatives of the ac transfer characteristics with respect to the input voltage v_{b2e1} .

The small-signal definitions of the epilayer current and the main current in the Mextram implementation are

$$i_n = g_x \cdot v_{b2e1} + g_y \cdot v_{b2c2} \quad (1)$$

$$i_{epi} = g_{epiy} \cdot v_{b2c2} + g_{epiz} \cdot v_{b2c1} \quad (2)$$

where

$$g_x = \frac{\partial I_n}{\partial V_{b2e1}}, \quad g_y = \frac{\partial I_n}{\partial V_{b2c2}}, \quad g_{epiy} = \frac{\partial I_{epi}}{\partial V_{b2c2}}, \quad g_{epiz} = \frac{\partial I_{epi}}{\partial V_{b2c1}} \quad (3)$$

ac short circuiting the output for the given network topology yields: $v_{b2c1} = v_{b2e1}$ and $i_n = i_{epi}$. Using these conditions we can solve for the small-signal transconductance i_{epi}/v_{b2e1} , leading to

$$\frac{i_{epi}}{v_{b2e1}} = g_x + g_y \cdot \left[\frac{g_{epiz} - g_x}{g_y - g_{epiy}} \right] \quad (4)$$

Although appearing simple in its representation the conductances used in (4) represent very complicated functions. As

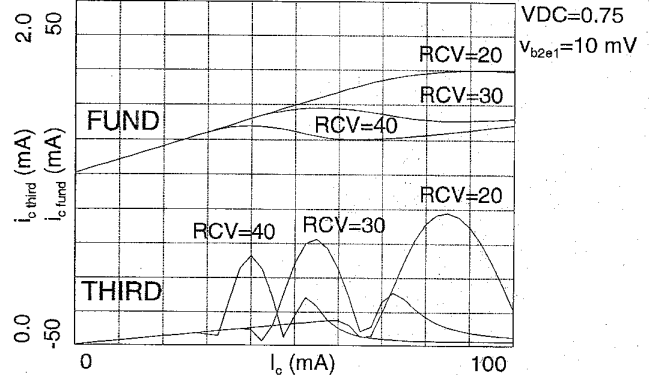


Fig. 8. The influence of RCV on the fundamental and third harmonic components.

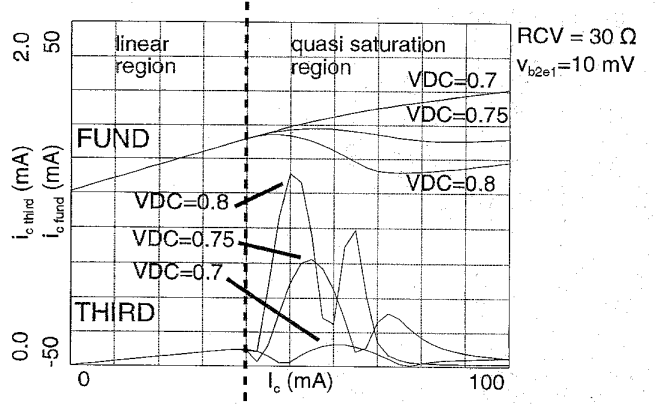


Fig. 9. The influence of VDC on the fundamental and third harmonic components when a transistor enters quasi-saturation.

we are interested in the influence of the epilayer parameters on the distortion behavior at the onset of q.s, we ignore (for this analysis only) the influence of the normalized base charge component (high injection, Early effect) and simplify the conductances to their first order approximation.

No Saturation: In this situation the main current is given by

$$I_n = I_f = I_s \cdot \exp(V_{b2e1}/V_t)$$

consequently $g_x = I_f/V_t$ (linear with the collector current) and $g_y \approx 0$.

Quasi-Saturation ($V_{b2c2} > 0$): In this situation the main current is given by

$$I_n = I_f - I_r = I_s \cdot (\exp(V_{b2e1}/V_t) - \exp(V_{b2c2}/V_t))$$

consequently $g_x = I_f/V_t$, $g_y = -I_r/V_t$, and $g_x + g_y = I_n/V_t$.

Considering the transconductance of (4) as function of the dc collector current we note that i_{epi}/v_{b2e1} in the non-saturated region equals g_x and is linear with the dc collector current. When entering q.s, g_y is no longer zero and the transconductance no longer increases linearly (see curves marked with "fund")-(amental) in Figs. 8 and 9). The higher harmonics (2nd and 3rd) can be determined from the derivatives of the transconductance with respect to V_{b2e1} .

Low frequency distortion measurements

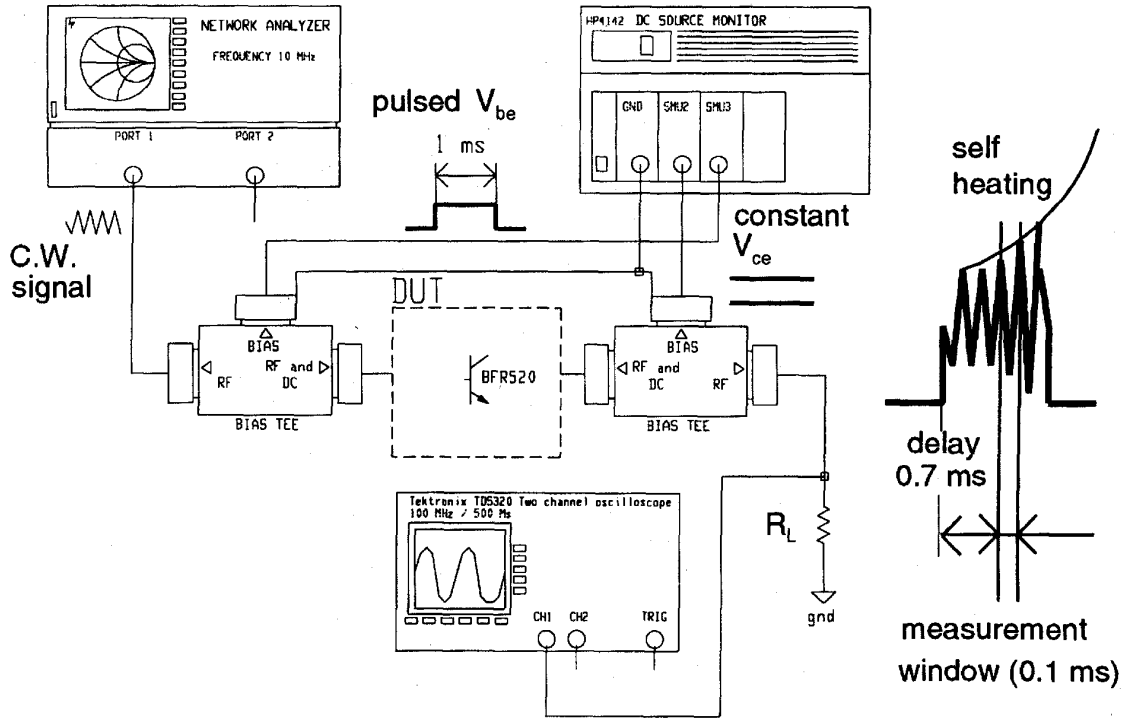


Fig. 10. Low frequency distortion measurement setup using a 100 MHz/500 megasamples/s oscilloscope.

The Influence of the Parameters VDC and RCV

For reasons of simplicity we will use the Kull model [11] with a purely ohmic epilayer description, neglecting hot carrier effects (the Kull model in any case becomes inaccurate when approaching IHC). This simplified Kull model is equal to the Mextram model for low current values and has the advantage for this analysis that I_{epi} is only affected by two parameters (see Appendix): RCV, which represents the epilayer resistance, and VDC (the built-in base collector junction voltage). RCV will influence the value of the collector current at which the internal junction becomes forward biased for a given external base collector voltage (see Fig. 8). In contrast, the built-in voltage VDC hardly affects the current at which the transistor enters q.s, but it will determine how much the internal base collector junction will become forward biased and thus directly determines g_y . The value of g_y acts as weighting factor for the term between brackets in (4) and it affects the slope of the decrease of the transconductance. This is of major importance for the increase in distortion when the device enters the q.s. region. In summary, we note that a device with a high built-in junction voltage will result in more distortion when it enters q.s. than a similar device with a lower built-in voltage. This is illustrated in Fig. 9.

In the standard Mextram parameter extraction the epilayer parameters RCV, VDC, IHC, SFH, and SCRCV are found by fitting both the $f_T(I_c)$ fall-off and the q.s. region of the $I_c(V_{ce})$ characteristics (see shaded area Fig. 6). This will give

a good first order approximation of the epilayer parameter values, fine tuning for accurate harmonic description can be performed by concentrating on the fit of the transconductance as a function of I_c for several base collector voltages in the frequency range of interest.

IV. SIMULATION AND MEASUREMENTS RESULTS AT LOW FREQUENCIES

Simulations: The calculated distortion data for the BFR520 has been obtained using our Mextram implementation in Hewlett Packard's harmonic balance simulator MDS. This has proven to be a particularly valuable tool in this investigation.

Measurements: Although pulsed bias voltages are applied to minimize self heating effects, the device under test (DUT) will generally heat-up within 0.1 ms, leading to an increase in the collector current. To avoid corruption of the distortion data the LF measurement should be short in time and take place at exactly the same moment when the bias current I_c is measured. At lower current levels distortion measurements can be carried out using a spectrum analyzer (SPA). At higher current levels self heating of the DUT will give temperature-related errors due to the minimum sweep time (e.g., 20 ms) inherent to the instrument. In principle, faster measurements are possible by setting the SPA to zero bandwidth and locking the signal source to the SPA. In practice, SPA (hp8566A) firmware related problems made it impossible to achieve the desired measurement time (e.g., $t < 0.1$ ms).

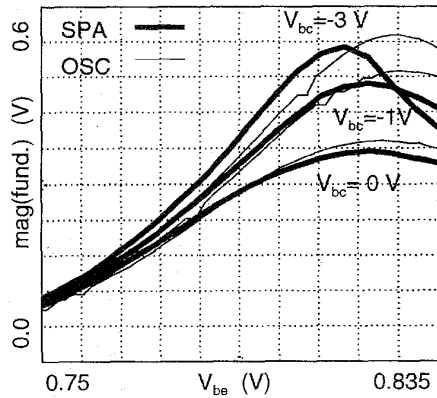


Fig. 11. Comparison of data obtained with a SPA (20 ms) and sampling scope (1 ms).

Alternatively, distortion measurements can be carried out using a 100 MHz, 500 megasamples/s data acquisition scope to maintain the phase information. An illustration of this measurement setup is given in Fig. 10. The network analyzer is used as a 10 MHz signal source. At a constant V_{ce} , the V_{be} of the transistor is pulsed for 1 ms. The amplified signal will stabilize at the output of the DUT within $50 \mu\text{s}$ and the sample scope triggered. Following a delay of approximately 0.7 ms, the dc collector current as well as the ac voltage over the 50 ohm load resistance during a time span of 0.1 ms are measured and read by HP's data acquisition program VEETEST. For each bias point, a trace of the load resistance voltage is taken and a fast Fourier transformation (FFT) is performed to find the coefficients of the distortion components. Since a large number of periods are measured the FFT will work as an averaging filter, leading to improved accuracy. The measurement results obtained using a SPA and a sample scope are compared in Fig. 11. The results of the SPA drift away at higher collector base voltages as the DUT consumes more power.

Results: In comparing Mextram to Gummel-Poon simulations, we note that the third order distortion maximum is manifest when approaching the $V_{b2c2} \approx 0.7 \text{ V}$ lines of Fig. 6. Since in the case of Gummel-Poon this line is reached much later, bipolar transistor distortion at higher current levels is improperly modelled (see Figs. 12–14 for increasing drive voltages). In these figures the amplitude of the fundamental frequency (10 MHz) as well as the second and third order distortion components of the collector voltage are plotted as a function of I_c for $V_{bc} = 0, -1, \text{ and } -3 \text{ V}$. (The ac collector voltage is directly related to the ac collector current via a 50 ohm load resistor).

In general, the distortion of larger signals is more easily modelled because small details in the device characteristics are then of reduced significance.

V. DISCUSSION AND LOW FREQUENCY RESULTS

Comparison of the measured and simulated low frequency (LF) distortion results leads to the conclusion that Mextram is far more accurate than GP at all power levels. At higher power

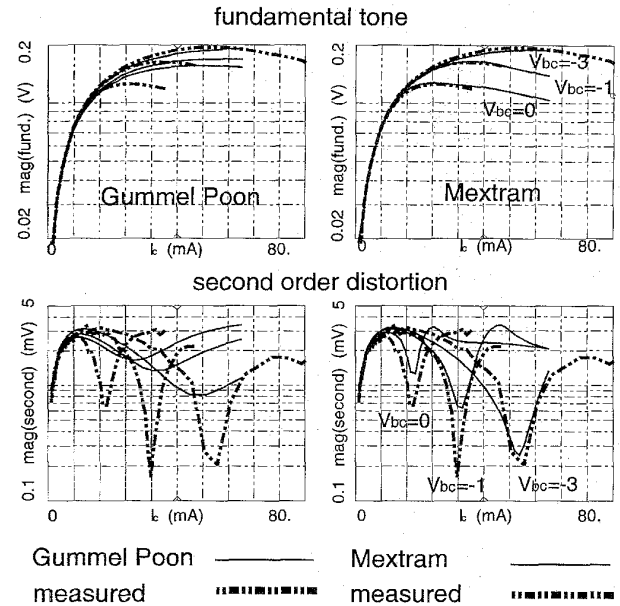


Fig. 12. Simulated and measured distortion components in the collector voltage of the BFR520 at a driving input voltage of 7 mV.

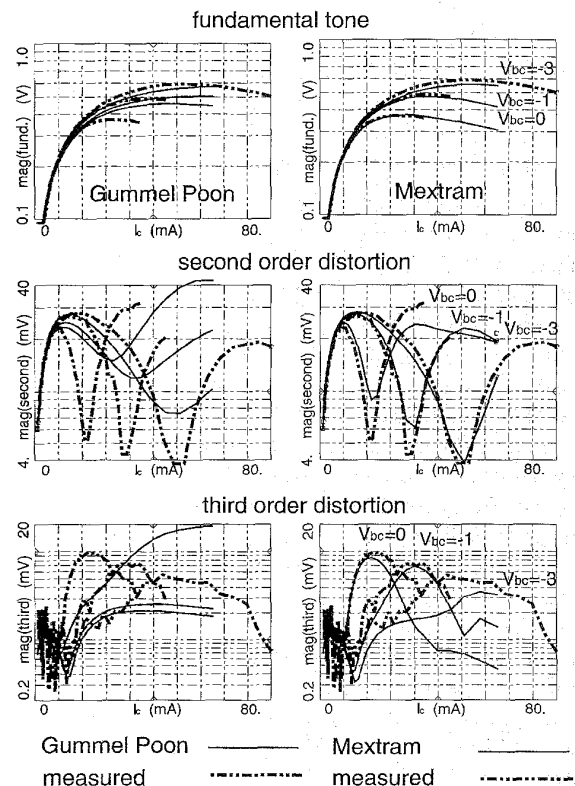


Fig. 13. Simulated and measured distortion components in the collector voltage of the BFR520 at a driving input voltage of 21 mV.

levels the fit for GP seems to improve somewhat, due to the fact that the transistor now enters hard saturation increasing

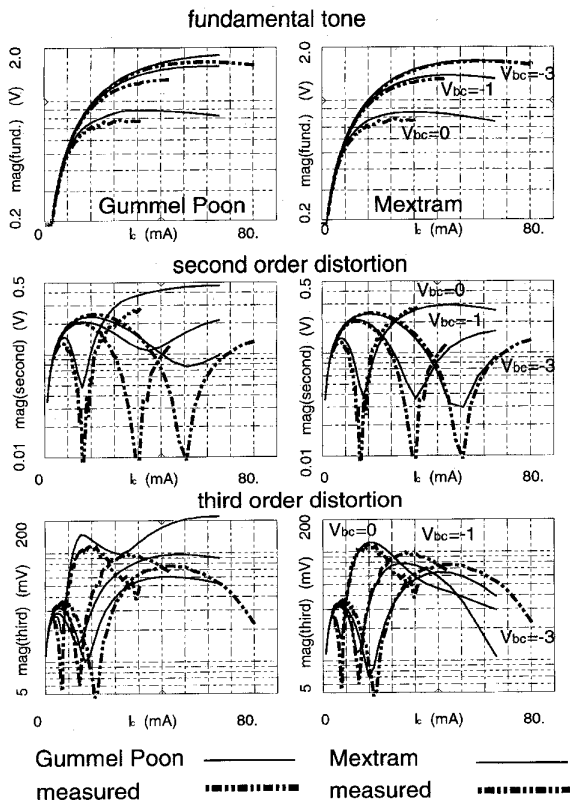


Fig. 14. Simulated and measured distortion components in the collector voltage of the BFR520 at a driving input voltage of 62 mV.

the third order distortion. In Fig. 14 we note that although there is a better fit for the third order distortion, the minima are still dislocated with respect to the collector current. Second order distortion products as predicted by the GP model fail as well to describe the measured results.

VI. HIGH CURRENT HIGH FREQUENCY DISTORTION EFFECTS

In analyzing high frequency signal distortion in bipolar transistors, charge functions have to be taken into account. The distortion is attributable to an interaction of contributions caused by the nonlinear current sources (as described previously) and charges. In the previous analysis it was evident that the built-in voltage (V_{DC}) has a major influence on the distortion behavior at low frequencies. The same parameter V_{DC} is also very important in modeling the f_T fall-off at high current levels. In bipolar transistor models with an epilayer model based on a voltage-controlled current source, [11], [18] the choice of the parameter V_{DC} is very critical. A somewhat lower built-in voltage (e.g., 650 mV) can easily cause non-monotonic behavior of the $f_T(I_c)$ fall-off characteristic. In practice, one compromises during parameter extraction to avoid nonmonotonic behavior by choosing a somewhat higher value for the built-in voltage (e.g., $V_{DC} = 700$ mV). Doing so, however, increases the apparent distortion at the onset of q.s. and leads to improper modeling at high current levels.

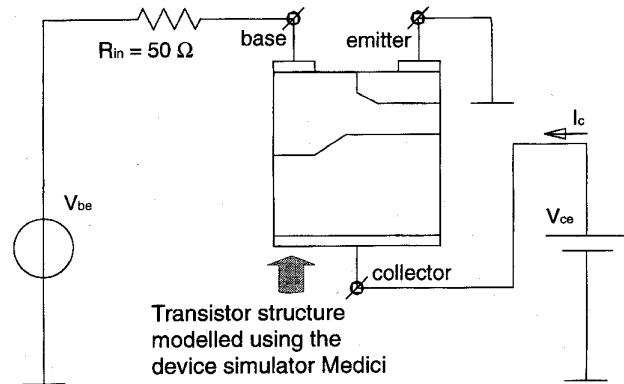


Fig. 15. Configuration used in the Medici calculations.

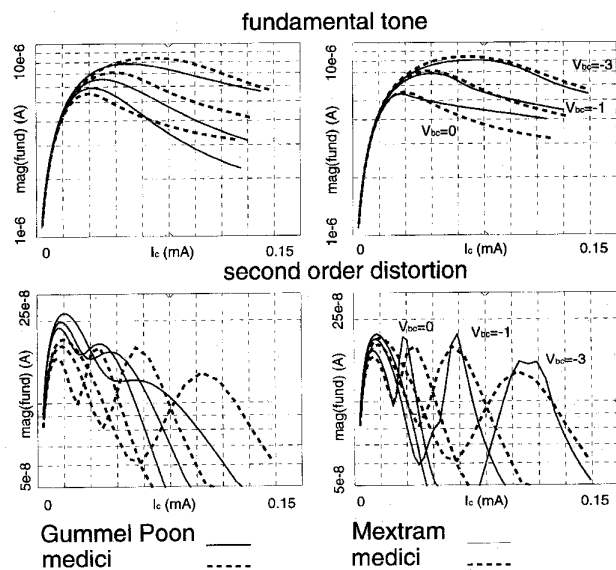


Fig. 16. Simulated distortion components in the collector current at a driving input voltage of 10 mV at 1 GHz.

To circumvent the problem above, an improvement to the modeling of the collector charge function, which enforces monotonic f_T fall-off and Early voltages for all parameter sets has been formulated. Implementation of this new collector charge expression in the Mextram model leads to better modeling of the distortion at the onset of quasi-saturation at higher frequencies. The improved collector charge description will be discussed in [20], in this paper we restrict ourselves to a summary of the final results.

Proper verification of distortion modeling requires comparative data. Obtaining accurate, reliable RF distortion data, while avoiding self-heating, proved, however, to be very troublesome with the equipment available. We have, therefore, in lieu of measurements used a 2-D device simulator Medici [21] to generate data as suggested in [17] for very large signal (almost switching) conditions. In our simulations we have used the transistor structure described in [17] which is based on SIMS measurements and is representative of present day bipolar

transistor technology. The configuration that has been used in the calculations is given in Fig. 15. Distortion results for a 10 mV, 1 GHz input signal, as obtained with the 2-D device simulator Medici and the modified Mextram model are given in Fig. 16.

VII. CONCLUSIONS

Incorporation of the latest developments in the formulation of epilayer behavior in Mextram, has provided a compact transistor model capable of accurately describing the distortion behavior of a transistor when operation extends into the region of quasi-saturation. Implementation of Mextram in the simulator package MDS has resulted in a very powerful combination facilitating the use of harmonic balance techniques in strongly non-linear circuit design. The results of this paper are verified by experiments for LF conditions. When considering RF excitation the charge functions must also be taken into account. A modification to the (standard 503) Mextram model ensuring f_T fall-off monotonicity, and concomitantly improved modeling of distortion under RF conditions, will be published shortly [20].

APPENDIX EPI-LAYER MODELS

The Epilayer Current Formulation in the MEXTRAM Model

The derivation of the MEXTRAM epilayer model may be found in [18]. The epilayer current is given by

$$I_{\text{epi}} = I_{\text{low}} + \text{SFH} \cdot \frac{V_{c1c2} - I_{\text{low}} \cdot \text{RCV} \cdot \left(1 - \frac{X_i}{W_{\text{epi}}}\right)}{\text{SCRCV} \cdot \left(1 - \frac{X_i}{W_{\text{epi}}}\right)^2} \quad (\text{A.1})$$

with

$$I_{\text{low}} = \frac{\text{IHC} \cdot V_{c1c2}}{V_{c1c2} + \text{IHC} \cdot \text{RCV} \cdot \left(1 - \frac{X_i}{W_{\text{epi}}}\right)} \quad (\text{A.2})$$

$$\frac{X_i}{W_{\text{epi}}} = \frac{E_c}{I_{\text{epi}} \cdot \text{RCV}} \quad (\text{A.3})$$

E_c is defined as

$$E_c = V_t \left(K_O - K_W - \ln \frac{K_O + 1}{K_W + 1} \right) \quad (\text{A.4})$$

with

$$K_O(V_{b2c2}) = \sqrt{1 + 4 \cdot \exp[(V_{b2c2} - \text{VDC})/V_t]} \quad (\text{A.5})$$

$$K_W(V_{b2c1}) = \sqrt{1 + 4 \cdot \exp[(V_{b2c1} - \text{VDC})/V_t]} \quad (\text{A.6})$$

where

X_i/W_{epi}	Normalized thickness of the injected region of the epilayer.
SFH	Factor for the epilayer current spreading.
IHC	Critical current density for hot carriers.
RCV	Ohmic epilayer resistance.

SCRCV	Space-charge limited epilayer resistance.
VDC	Built-in voltage of the base collector
V_t	Thermal voltage.

SFH, IHC, RCV, and SCRCV are Mextram model parameters [18], [19]. Substitution of (A.2) and (A.3) in (A.1) and solving for I_{epi} will lead to a cubic equation. Complete implementation of the Mextram model is described in [19].

The Epilayer Current According to the Kull Model

Neglecting hot carriers the Mextram epilayer current model reduces to the simplified Kull model for the ohmic case. This can be found by letting IHC go to infinity in (A.2) and by substitution of (A.2) into (A.1), leading to $I_{\text{epi}} = I_{\text{low}}$. With the help of (A.3) we find

$$I_{\text{epi}} = \frac{E_c + V_{c1c2}}{\text{RCV}} \quad (\text{A.7})$$

The complete Kull model [11] including hot carrier effects has an additional term in the denominator

$$I_{\text{epi}} = \frac{E_c + V_{c1c2}}{\text{RCV} + \frac{|V_{c1c2}|}{\text{IHC}}}$$

ACKNOWLEDGMENT

The authors wish to thank W. Kloosterman, M. Versleijen, and L. Harms of Philips Research and Philips Semiconductors respectively for their support of the project and W. Krans and W. Eisinga of the Laboratory of Electrical Materials for the use and support of the device simulation program Medici.

REFERENCES

- [1] C. T. Kirk, "A theory of transistor cut-off frequency (f_T) fall-off at high current densities," *I.R.E. Trans. Electron Devices*, vol. ED-9, p. 164, 1962.
- [2] J. Reynolds, "Nonlinear distortions and their cancellation in transistors," *IEEE Trans. Electron Devices*, no. ED-11, pp. 595-599, Nov. 1965.
- [3] S. Narayanan, "Transistor distortion analysis using volterra series representation," *Bell Syst. Tech. J.*, vol. 40, 1967.
- [4] J. R. A. Beale and J. A. G. Slatter, "The equivalent circuit of a transistor with a lightly doped collector operating in saturation," *Solid-State Electr.*, vol. 11, p. 241, 1968.
- [5] J. A. Pals and H. C. de Graaff, "On the behavior of the base-collector junction of a transistor at high collector current densities," *Philips Res. Rep.* 24, p. 53, 1969.
- [6] L. A. Hahn, "The effect of collector resistance upon the high current capability of n-p-n transistors," *IEEE Trans. Electron Devices*, vol. ED-16, p. 654, 1969.
- [7] D. L. Bowler and F. A. Lindholm, "High current regimes in transistor collector regions," *IEEE Trans. Electron Devices*, vol. ED-20, p. 257, 1973.
- [8] S. Narayanan and H. C. Poon, "An analysis of distortion in bipolar transistors using integral charge control model and volterra series," *IEEE Trans. Circuit Theory*, vol. CT-20, no. 4, July 1973.
- [9] H. C. de Graaff and R. J. van der Wal, "Measurement of the onset of quasi saturation in bipolar transistors," *Solid-State Electron.*, vol. 17, pp. 1187-1192, 1974.
- [10] L. J. Tureon and J. R. Mathews, "A bipolar transistor model of quasi-saturation for use in CAD," *IEDM Tech. Dig.*, 1980, p. 394.
- [11] G. M. Kull, L. W. Nagel, S. W. Lee, P. Lloyd, E. J. Prendergast, and H. Dirks, "A unified circuit model for bipolar transistors including quasi-saturation effects," *IEEE Trans. Electron Devices*, vol. ED-32, pp. 1103-1113, June 1985.
- [12] P. Antognetti and G. Massobrio, *Semiconductor Device Modelling with SPICE*. New York: McGraw-Hill, 1987.

- [13] H. Jeong and J. G. Fossum, "Physical modeling of high-current transistors for bipolar transistor circuit simulation," *IEEE Trans. Electron Devices*, vol. ED-34, p. 898, 1987.
- [14] H. C. de Graaff and F. M. Klaasen, *Compact Transistor Modelling for Circuit Design*. New York: Springer-Verlag, 1990.
- [15] H. F. F. Jos, "A model for the non-linear base-collector depletion layer charge and its influence on intermodulation distortion in bipolar transistors," *Solid-State Electron.*, vol. 33, no. 7, pp. 907-915, 1990.
- [16] ———, "Collector model describing bipolar transistor distortion at low voltages and high currents," *Solid-State Electron.*, vol. 37, no. 2, pp. 341-352, 1994.
- [17] M. P. J. G. Versleijen and A. Bauvin, "Accuracy of bipolar compact models under RF power operating conditions," *IEEE MTT-S Tech. Dig.*, 1994, pp. 1583-1586.
- [18] H. C. de Graaff and W. J. Kloosterman, "Modelling of the collector epilayer of a bipolar transistor in the Mextram model," *IEEE Trans. Electron Devices*, vol. 42, no. 2, pp. 274-282, Feb. 1995.
- [19] ———, *The Mextram Bipolar Transistor Model*, 1993, (implementation guide available on request from Philips Research Laboratories, P.O. Box 80000, 5600 JA Eindhoven, The Netherlands.)
- [20] L. C. N. de Vreede, H. C. de Graaff, J. L. Tauritz, and R. G. F. Baets, "Extension of the collector charge description for compact bipolar models," presented at *ESSDERC '95*, The Hague, The Netherlands.
- [21] Medici, Two-Dimensional Device Simulation Program, version 1.1, Technolgy Modeling Associates Inc., Mar. 1993.



Leo C. N. de Vreede was born in Delft, The Netherlands in 1965. He received the B.S. degree in electrical engineering from the Hague Polytechnic in 1988.

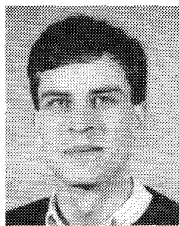
In the summer of 1988 he joined the Microwave Component Group of the Laboratory of Telecommunication and Remote Sensing Technology of the Department of Electrical Engineering, Delft University of Technology. From 1988 to 1990 he worked on the characterization and modeling of CMC capacitors. Mr. de Vreede is currently carrying out

Ph.D. research on the hierarchical design of silicon MMIC's.



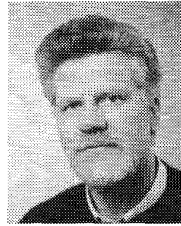
Henk C. de Graaff was born in Rotterdam, The Netherlands, in 1933. He received the M.Sc. degree in electrical engineering from Delft University of Technology in 1956 and the Ph.D. degree from the Eindhoven University of Technology, in 1975.

He joined Philips Research Laboratories, Eindhoven, in 1964 and has been working on thin-film transistors, MOST, bipolar devices, and materials research on polycrystalline silicon. His present field of interest is device modeling for circuit simulation. Since his retirement from Philips Research (November 1991) he has been a consultant to the University of Twente and the Delft University of Technology, both in The Netherlands.



Koen Mouthaan (S'94) was born in Voorburg, The Netherlands, in 1967. He received the M.Sc. degree in electrical engineering from Delft University of Technology, Delft in 1993.

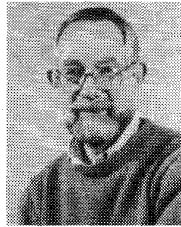
Mr. Mouthaan is currently carrying out Ph.D. research on the modeling of RF high power bipolar transistors.



Marinus de Kok was born in the Hague, The Netherlands in 1942. He graduated from the Dutch Air Force Electronic School in 1963 and received the B.S. degree in electrical engineering from the Polytechnic Institute of the Hague in 1967.

Mr. de Kok joined the technical staff of the Department of Electrical Engineering, Delft University of Technology in 1966. In 1976 he became a member of the Microwave Component Group of the Laboratory of Telecommunication and Remote Sensing Technology (formerly Microwave Laboratory). His

work is primarily concentrated on the development and implementation of state of the art microwave measurement and modeling software within a UNIX environment.



Joseph L. Tauritz (S'60-M'63) was born in Brooklyn, NY in 1942. He received the B.E.E. degree from New York University in 1963 and the M.S.E. degree in electrical engineering from the University of Michigan in 1968. He was a research fellow at the Delft University of Technology from 1970 to 1971.

He first became acquainted with microwaves while working as a junior engineer on circularly polarized antennas at Wheeler Labs in the summer of 1962. From 1963 to 1970 he worked as a

technical specialist attached to the R.F. department of the Conduction Corporation where he designed innovative microwave, VHF, and video circuitry for use in high resolution radar systems. In 1970 he joined the scientific staff of the Laboratory of the Telecommunication and Remote Sensing Technology of the Department of Electrical Engineering, Delft University of Technology, where he is presently an assistant professor. Since 1976 he has headed the Microwave Component Group where he is principally concerned with the systematic application of computer aided design techniques in research and education. His interests include the modeling of high frequency components for use in the design of MIC's and MMIC's, filter synthesis, and planar superconducting microwave components.

Mr. Tauritz is a member of Eta Kappa Nu and the Royal Dutch Institute of Engineers.



Roel G. F. Baets (M'88) received the degree in electrical engineering from the University of Gent, Belgium, in 1980. He received the M.Sc. degree in electrical engineering from Stanford University in 1981 and the Ph.D. degree from the University of Gent in 1984.

Since 1981 he has been with the Department of Information Technology of the University of Gent. In 1989 he was appointed Professor in the engineering faculty of the University of Gent and in 1990 he received a part-time appointment at the

Delft University of Technology as well. He has worked in the field of III-V devices for optoelectronic systems. With over 100 publications and conference papers, he has made contributions to the modeling of semiconductor laser diodes, passive guided wave devices and to the design and fabrication of OEIC's. His main interests are now in the modeling, design and testing of optoelectronic devices, circuits and systems for optical communication, and optical interconnects.

Dr. Baets is a member of the Optical Society of America and the Flemish Engineers Association. He has served as a member of the program committee of the ESSDERC Conference of the IEEE International Laser Conference and of the ECOC Conference.